

# **Hardening of Arches for Commercial Simulation of Industrial Flares: A Second Program Update**

Minmin Zhou, Marc Cremer  
Reaction Engineering International  
zhou@reaction-eng.com, cremer@reaction-eng.com

Jennifer Spinti  
University of Utah  
Jennifer.Spinti@utah.edu

This paper will provide an update to our US Department of Energy funded program that is focused on leveraging the Uintah Computational Framework (UCF), originally developed at the University of Utah, for commercial simulation of industrial flares. The Arches component of the UCF provides a reacting large eddy simulation (LES) capability, which is a more fundamentally accurate description of turbulent mixing and combustion than is obtained in conventional Reynolds Averaged Navier Stokes (RANS) approaches. Our paper from last years' conference described the results of two simulations of the air-assist flare of the Texas Commission on Environmental Quality (TCEQ) flare study as well as the results from simulations of pilot scale multipoint ground flare tests.

This paper focuses on the following two project results:

- Arches LES simulations of TCEQ steam-assist flare operation
- Arches LES simulation of air-assist operation carried out through the web-based interface running on the Nimbix HPC cluster

The completed steam-assist flare simulations focused on the S2.1 and S2.5 tests from the TCEQ 2010 study. The primary difference between these two test cases is the ratio of steam flow to vent gas flow rate: 1) S2.1, Ratio = 2.3; 2) S2.3, Ratio = 5.4. The Arches LES simulations were in good quantitative agreement with the results of the TCEQ tests showing a significant reduction in the measured combustion efficiency from 99.4% to 83.5%. The details of the steam-assist flare tests and the corresponding results of the simulations will be presented.

A significant focus of our program has been the development of a front-end and back-end web-based interface for case definition, simulation, monitoring, and post processing of Arches simulations. We will describe the results of the demonstration of the web-interface on simulation of one of the air-assist operational conditions from the TCEQ flare study running on the Nimbix HPC cluster.

## 1 Introduction

Flares are used at chemical plants and petroleum refineries as a control device for regulated vent streams as well as to handle non-routine emissions (e.g., leaks, purges, emergency releases). In conjunction with experimental measurements, high-fidelity CFD simulations can provide significant insight into the behavior of industrial flare systems. REI has been collaborating with researchers at the University of Utah to apply Arches/Uintah to simulation of industrial flares [1, 2, 3]. During the last year, this program has focused on development of flare library templates for the simulation of two steam-assisted flare operating conditions.

The two steam-assisted operational conditions (S2.1 and S2.3) are from the 2010 Texas Commission on Environmental Quality (TCEQ) study [4, 5]. The reason for these two selections is that the two operational conditions utilized significantly differing steam assist flow rates, which experimentally yielded significant differences in combustion efficiency. Specifically, the steam-assisted rate in the S2.3 test is about two-fold that of the S2.1 test. The experimental data indicated that over-steaming can significantly reduce the flare combustion efficiency. We applied Arches to these operating conditions to investigate the predicted impact of steam-assist rate on combustion efficiency.

One challenge for steam-assisted flare simulations is to resolve the small length scales associated with the steam inlets which requires a significant amount of grid resolution. Due to Arches' uniform mesh, this could translate to an excessive run-time/cost requirement. Instead of directly resolving the steam inlet, we have utilized a "hand-off" strategy, which pre-defines the steam inlet velocity field around the steam inlet structure while conserving mass and momentum [6].

In addition to our development of a flare template library, our program has focused on development of a web-based interface to make Arches more accessible to potential users. We have focused our demonstration of the web-interface to the setup, simulation, and post processing associated with the TCEQ air-assisted case A2.4, accessing the Nimbix commercial HPC hardware. Our demonstration shows the overall functionality of the web-based interface.

## 2 Methods, Assumptions, and Procedures

### 2.1 Steam-assisted Flare Simulations

Two steam-assist flare cases from the TCEQ 2010 study have been the focus of recent work. The operating conditions of S2.1 and S2.3 in the TCEQ 2010 study are listed in Table 1. Combustion efficiencies for the various flare test conditions during the TCEQ study were based on two approaches: 1) remote sensing using Passive and Active Fourier Transform Infrared (PFTIR) spectroscopy, and 2) gas chromatographic (GC) analysis of extracted plume samples by Aerodyne Research, Inc. (ARI). Figure 1 shows the full-scale simulation domain (2.8 m, 6.0 m, 9.6 m). The length of the domain (y direction = wind direction) was 6.3 times of the diameter of the base of the flare (e.g., 0.9 m). The width of the domain (x direction = transverse direction) was 3 times of the diameter of the base of the flare. The height of the domain (z direction) was 2.3 times of the flare height (4.17 m).

**Table 1: Steam-assist operating conditions from 2010 TCEQ study**

	<b>S2.1</b>	<b>S2.3</b>
<b>Fuel</b>	Propylene	Propylene
<b>Fuel Flow Rate (lb/hr)</b>	937	937
<b>Fuel Initial Temperature (F)</b>	95	95
<b>Fuel Tip Velocity (ft/sec)</b>	0.95	0.95
<b>Steam Assist Flow Rate (lb/hr)</b>		
<b>Center Assist flow (lb/hr)</b>	540	543
<b>Upper Assist flow (lb/hr)</b>	1617	4651
<b>Total Steam Assist Flow Rate (lb/hr)</b>	2157	5195
<b>Wind Velocity (fps)</b>	8.3	8.1
<b>Combustion Efficiency</b>		
<b>PFTIR (%)</b>	99.4 ± 0.2	83.5 ± 10.6
<b>ARI (%)</b>	98.7 ± 1.3	40.7 ± 28.8

In accordance with lessons from the previously completed mesh sensitivity, the cell size of this simulation is approximately 0.02 m [3]. Also, this work employs the sigma subgrid-scale model [7]. This steam-assisted flare employs a continuous pilot. Our representation of the pilot is consistent with that which was previously described for the previously completed air-assisted flare simulation [2]. Although the pilot fuel differs in composition from that of the flare gas, limitations of the existing combustion model in Arches requires us to approximate the pilot gas composition as identical to that of the flare gas.

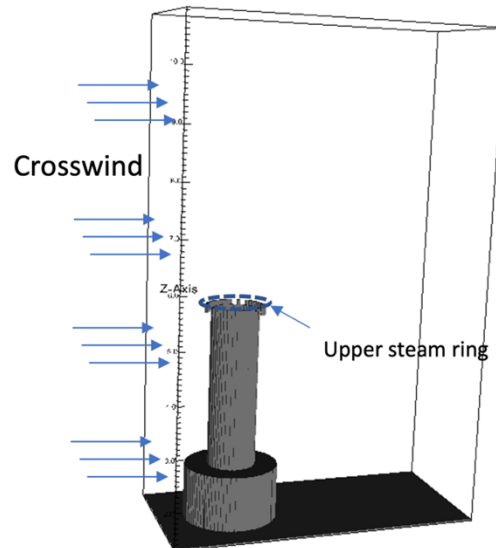


**Figure 1: Full-scale simulation domain for steam-assisted flare**

If CO<sub>2</sub> in the air is assumed to be negligible, our calculation of combustion efficiency (CE) is based on Eq. 1 below:

$$CE(\%) = \left( \frac{CO_2(plume)}{CO_2(plume)+CO(plume)+3*\sum C_3H_6(plume)} \right) \times 100, \quad \text{Eq. 1}$$

where, CE (%) = combustion efficiency (%); CO<sub>2</sub> (plume) = volume concentration of carbon dioxide in the plume (ppmv) after combustion has ceased; CO (plume) = volume concentration of carbon monoxide in the plume (ppmv) after combustion has ceased;  $\sum$ hydrocarbons (plume) = volume concentration of all the unburned hydrocarbons in the plume after combustion has ceased multiplied by the number of carbons in the hydrocarbon (ppmv).

In the TCEQ study a flare plume sampling system was used to continuously draw as large a sample of the plume as possible [8]. The plume gases were then analyzed using gas chromatography, to compute the CE per Eq. 1. Consistent with that approach, we have computed CE by integrating the gas concentrations over the model exits where the plume is defined based on mixture fraction > 1 ppmv. The integrated mass flow rates of the gas species at outlet boundaries of the simulation domain are used for the CE computation based on Eq. 1. Figure 2 shows an example of the CO<sub>2</sub> distribution at the model exits, subject to the mixture fraction criterion.

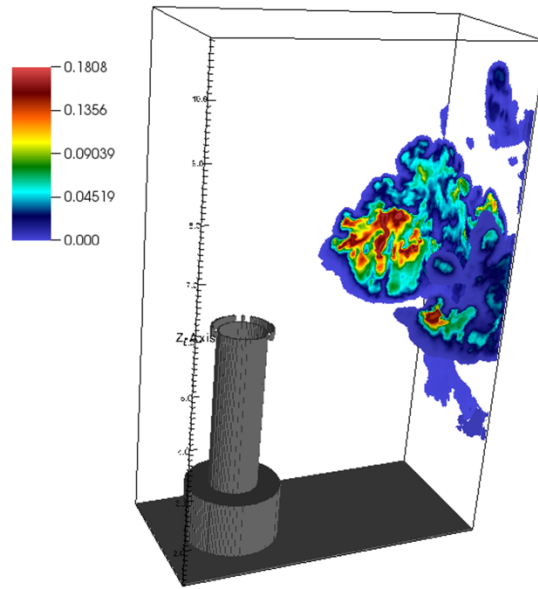


**Figure 2: CO<sub>2</sub> distribution subset by 1 ppmv mixture fraction criterion at the three outlets of the simulation domain**

## 2.2 Web User-Interface

The web user-interface (UI) that we have constructed acts like a single page application (e.g., Google Docs or Microsoft Office Online), which operates and behaves more like traditional desktop applications without the installation process. This user-interface uses JavaScript code and can run in any modern web browser. The UI consists of front-end and back-end parts, which allow the user to complete the key steps for a flare simulation: 1) the case setup, 2) simulation, 3) monitoring, and 4) post processing. The main workflow from UI to a CFD simulation is shown in Figure 3.

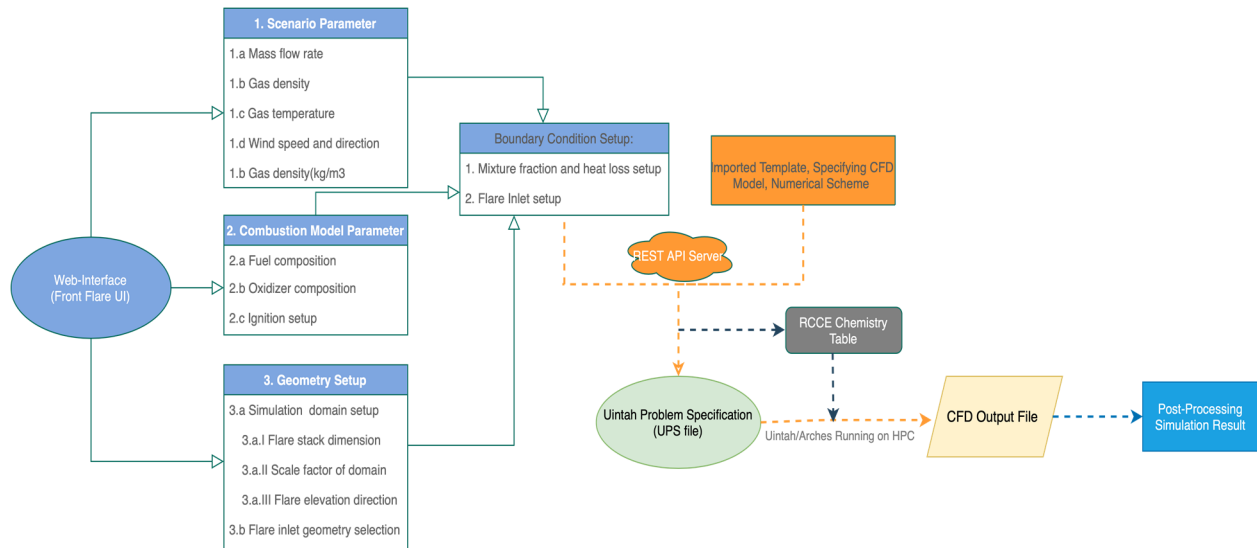


**Figure 3: Workflow from UI to CFD simulation**

The primary product of the front-end UI, with regards to the case setup, is the construction of the Uintah Problem Specification (UPS) file as the input file for the Arches simulation. The UPS file is written in Extensible Markup Language (XML) format, and it provides all the case setup information (inlet conditions, boundary conditions, geometry, numerical model parameters, etc.) that is necessary to execute an Arches simulation. Using Go programming language (by Google), we have developed the necessary code in the Flare API server (back-end) to interpret the information retrieved from the user’s input from the web-interface to output the correct UPS in the XML file format. In addition, the Flares API server generates an input file for the generation of the RCCE chemistry table on the HPC hardware, prior to execution of an Arches simulation.

After the finished case setup, the UI allows the user to specify HPC related parameters (number of CPUs, computational time, HPC location) via the implemented Docker container in the HPC Daemon Library. Monitoring of the simulation is achieved through transfer of the user-specified results from the HPC facility to the Flare API, with capability to plot results on the user browser. Once the simulation is completed, the user can download the data for subsequent post-processing [9].

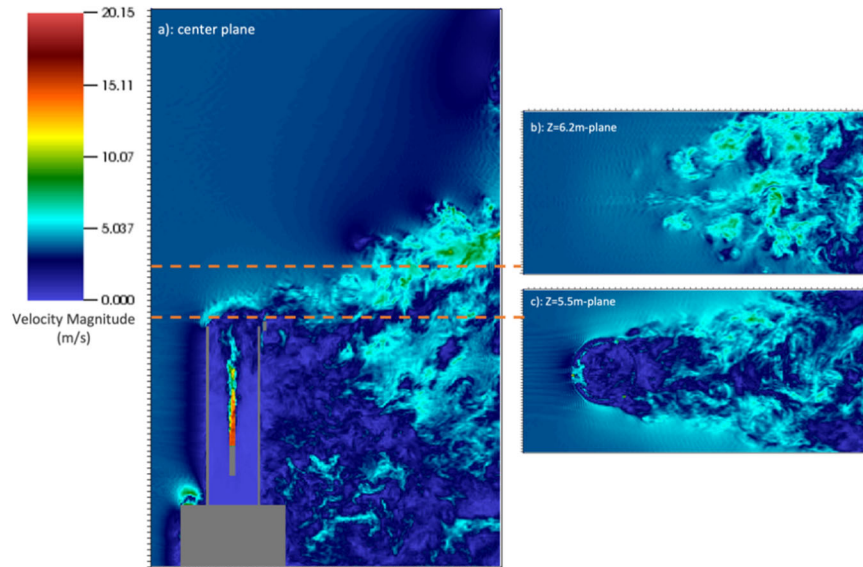
### 3 Results and Discussion

#### 3.1 Steam-assisted Flare Simulations

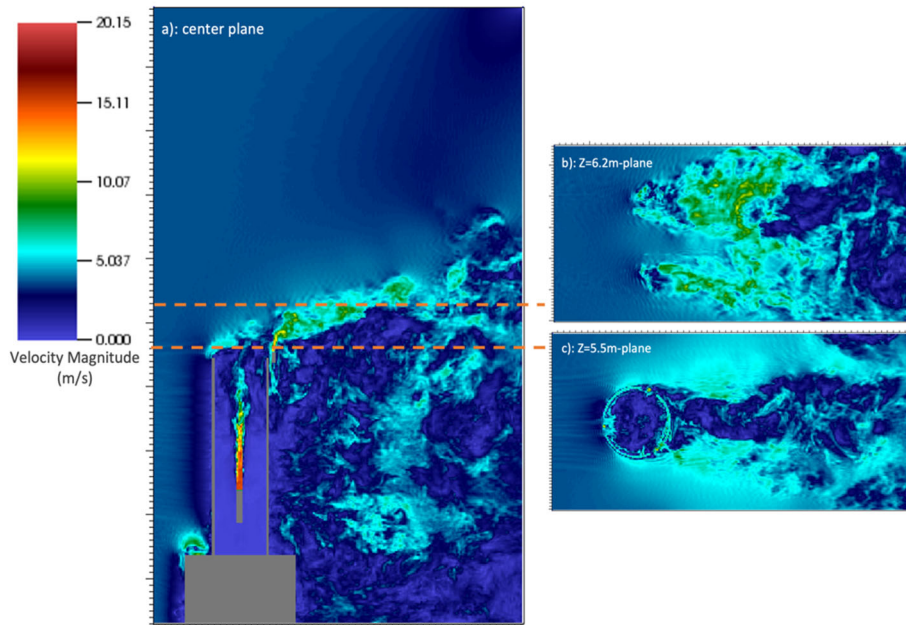
The focus of this section will be discussion of the results of the steam-assisted flare simulations, primarily role of steam rate on the predicted CE.

Figure 4 and Figure 5 show the instantaneous flow fields of S2.1 and S2.3 after the cases have become statistically stationary. To clearly present the velocity magnitude fields, three surfaces were selected as  $X=0$  m (center plane),  $Z=5.5$  m, and  $Z=6.2$  m. The center plane shows the vertical-injected vent gas bends horizontally due to the horizontal crosswind and simultaneously the plume is drawn upward. The center steam entrains the fuel and carries it vertically while the horizontal crosswind flows over the flare stack strips the vertical-injected fuel away from the flare stack. The

upper steam entrains the ambient air and increases the turbulence around the vent gas. Figure 4c and Figure 5c show the difference in velocity associated with the upper steam, where Figure 5c shows a light blue ring at the top of the flare stack representing the higher velocity of the upper steam for case S2.3. The increased vertical momentum of the upper steam in case S2.3 along with the increased buoyancy associated with the higher steam content results in somewhat less deflection of the flare plume, compared to case S2.1.



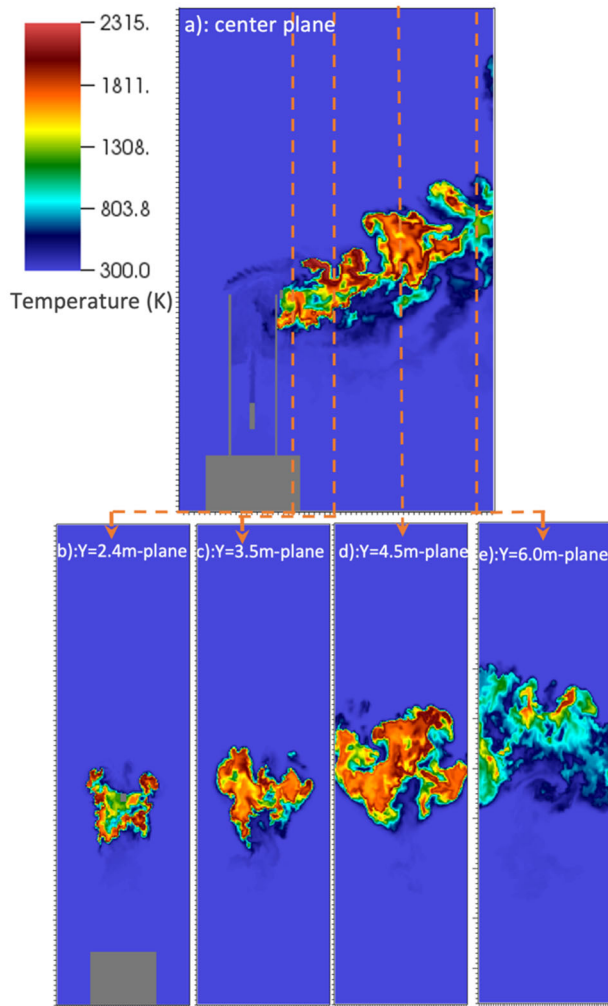
**Figure 4: Velocity magnitude (m/s) distribution for S2.1 flare simulation: a) center plane, b) Z=6.2 m plane, c) Z=5.5 m plane**



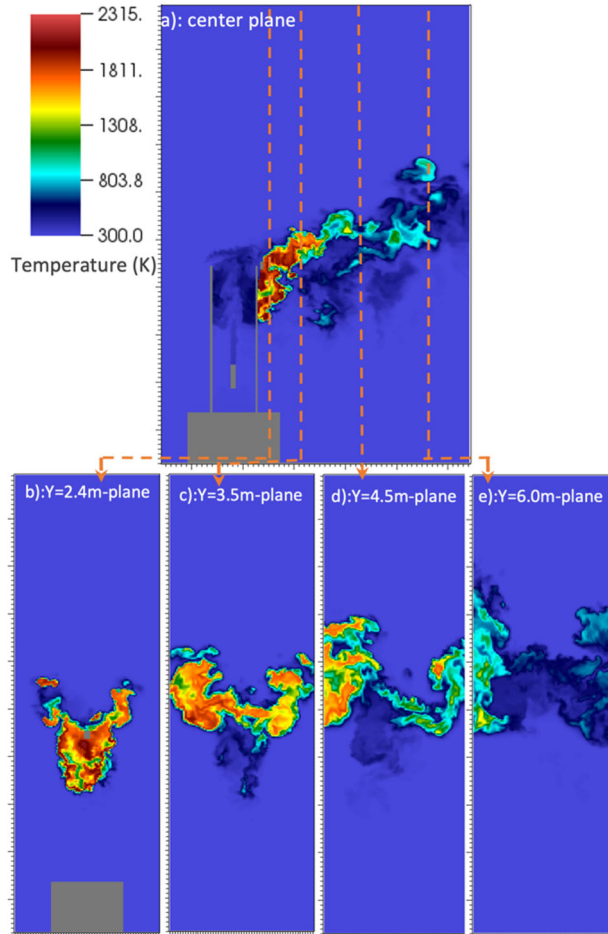
**Figure 5: Velocity magnitude (m/s) distribution for S2.3 flare simulation: a) center plane, b) Z=6.2 m plane, c) Z=5.5 m plane**

Figure 6 and Figure 7 show the instantaneous temperature fields of S2.1 and S2.3, respectively, after the cases have become statistically stationary. The figures show four cross-sectional planes to illustrate the evolution of flare development along the wind flow direction. (a) X=0 m, b) Y=2.4 m, c) Y=3.5 m, d) Y=4.5 m, e) Y=6.0 m. Comparison of the temperature distribution along the center plane for the two case results clearly shows higher temperatures throughout the flare plume, and extending further downstream in case S2.1. Comparison of the Y-plane profiles shows that the increased steam rate in case S2.3 leads to a more diffuse (i.e., wider) plume, as expected due to increased entrainment associated with the higher steaming rate.

Both results are consistent with observed behavior with steam-assist flares and impacts of over steaming. The increased steaming rate of case S2.3 reduces the net heating value in the combustion zone (NHVCZ), resulting in a reduction in the average temperature within the plume. However, the purpose of steam assist flares, to increase turbulent mixing between the flare gases and combustion air, generally increases combustion efficiency, until the reduced flare plume temperatures compensate for the benefits of increased turbulent mixing.



**Figure 6: Temperature distribution for S2.1 flare simulation: a) center plane (X=0 m plane), b) Y=2.4 m plane, c) Y=3.5 m plane, d) Y=4.5 m plane, e) Y=6.0 m plane**



**Figure 7: Temperature distribution for S2.3 flare simulation: a) center plane (X=0m plane), b) Y=2.4m plane, c) Y=3.5 m plane, d) Y=4.5 m plane, e) Y=6.0 m plane**

Figure 8 and Figure 9 show the predicted uncombusted fuel mass per volume distributions of S2.1 and S2.3, corresponding to the same instantaneous results shown in Figures 4 and 5. The profiles of fuel mass are useful in identification of mechanisms and locations for incomplete combustion. The center steam is injected at the center of flare stack effectively mixes with the fuel prior to exiting. For both cases, the cross wind strips a portion of the vertically injected fuel away from the flare stack, even below the top of the flare stack.

There are two apparent differences between the results for S2.1 and S2.3. First, there are eddies of significantly higher fuel concentration near the flare stack in S2.1 compared to S2.3, consistent with the higher steaming rate in S2.3, leading to increased dilution. Secondly, the center profile for S2.3 exhibits a more continuous, coherent structure of fuel in the center of the flare plume, while S2.1 shows more discrete parcels of fuel creating more surface area for mixing between the fuel parcels and air. Although the intention of the steam assist is to increase turbulence and mixing between the flare gases and air, these results indicate that over steaming with the upper steam injectors, may lead to less overall mixing between the fuel gases and air in addition to decreasing the rates of combustion due to the overall decrease in the NHVCZ.



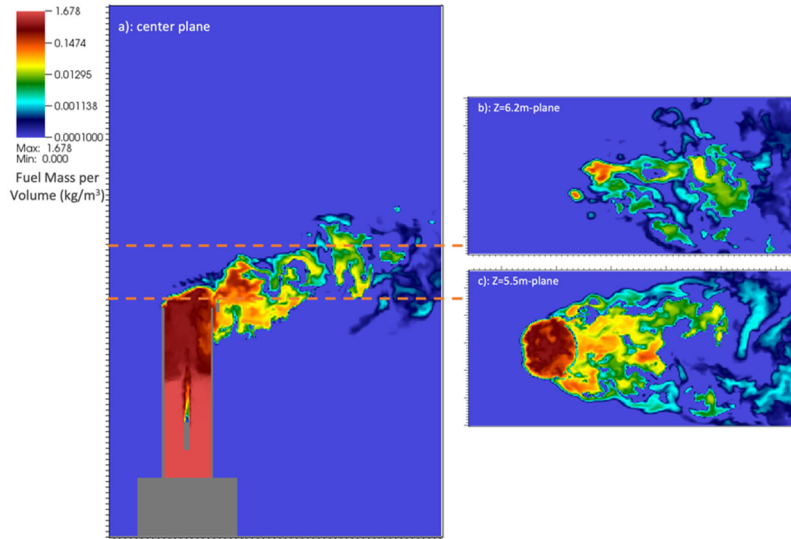


**Figure 8: Fuel mass per volume for S2.1 flare simulation: a) center plane, b) Z=6.2 m plane, c) Z=5.5 m plane**

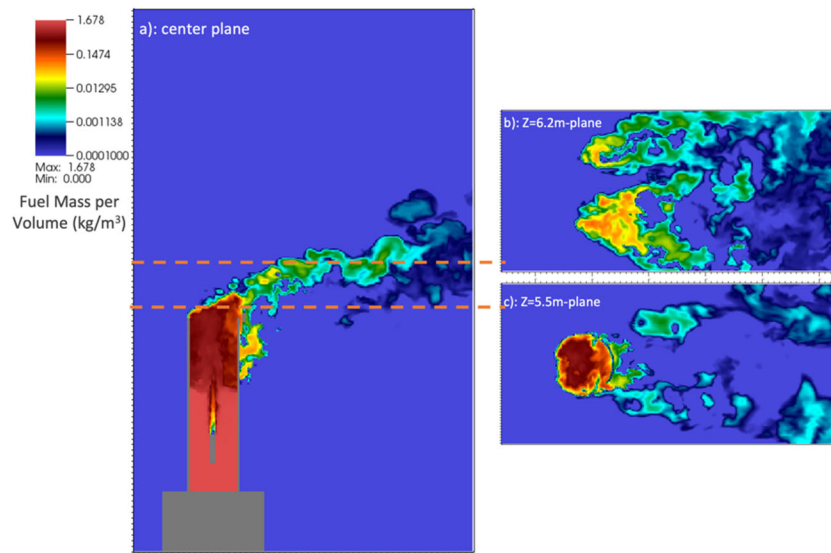


**Figure 9: Fuel mass per volume for S2.3 flare simulation: a) center plane, b) Z=6.2 m plane, c) Z=5.5 m plane**

Comparisons of the predicted combustion efficiency for simulations of S2.1 and S2.3, with the corresponding experimental data from the TCEQ tests are shown in Figure 10. The predicted time-averaged CE for S2.1 was 99.1%, relatively close to PFTIR measurement of 99.4% and the GC based measurements of 98.7%. For S2.3, about the predicted CE was 88.9%, a significant reduction compared to S2.1, and within 1 standard deviation of the PFTIR measurement of 83.5%. The GC based measurements of the extracted plume sample for this condition showed a significantly lower CE of 40.7% with a relatively large standard deviation of 28.8.

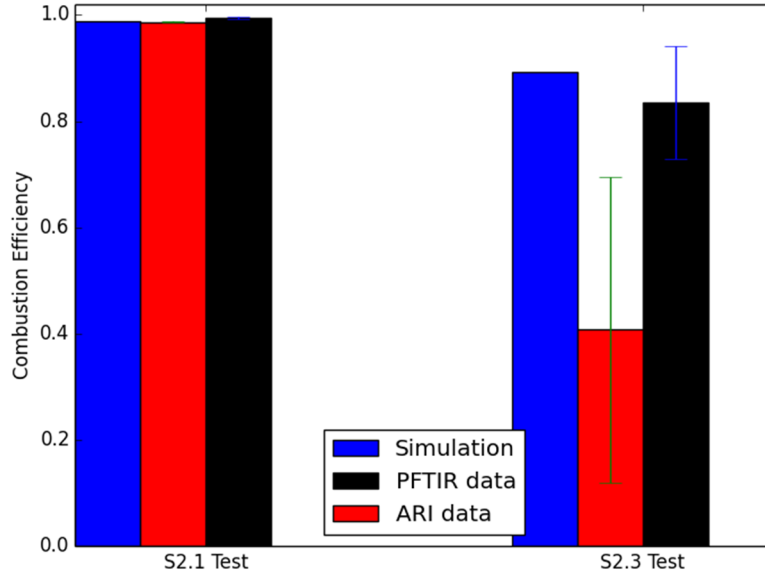


**Figure 10: Comparison between predicted and measured CE of two steam-assist conditions**

## 3.2 Flare Simulation Set-Up Through Web Interface

The web-based user interface can run in any modern browser and is being constructed to be fast and responsive. UI includes user login/registration and user permissions (i.e., a specific user is limited to access of their own files), and the login page is the entry point of the user to the application. The UI allows the user to create a new flare template from scratch or to start with an existing flare template, which resides in the library. The paradigm that we have used to design the UI allows for additional templates to be added with limited effort. Currently, four templates have been added, namely: Air-assisted-A21, Air-assisted-A24, Steam-assisted-S21, and Steam-assisted-S23, as is shown in Figure 11.

### 3.2.1 Template Selection

This study selected the air assisted A2.4 template as a demonstration case. Once a template is chosen, a new case set-up is generated and pre-filled with the template values. For example, when the TCEQ\_2010\_Air\_Assist\_A2.4 is selected, the geometry is automatically set to the corresponding flare tip (see Figure 12). The geometry preview pane features a 3D preview of the CAD geometry (STL format), which can be controlled with the mouse including the ability to orbit, pan, zoom, and rotate the 3D preview. The 3D geometry viewer is built on vtk.js which is a JavaScript implementation of the popular open source VTK (Visualization Tool Kit) library.

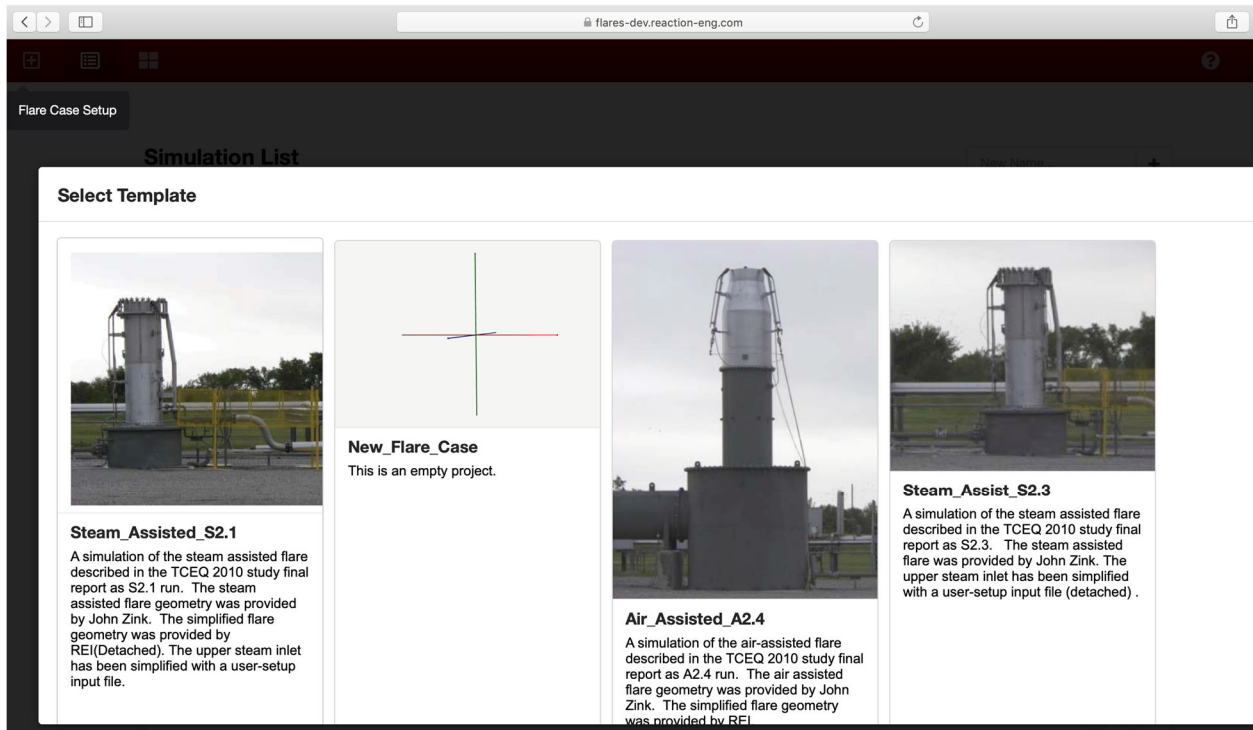


Figure 11: Template selection page

The user navigates through the various simulation set-up pages using the collapsible sidebar menu (see left side of Figure 12). Also, the web interface allows the user to define the simulation domain size in which each direction ratio button will automatically come up with the scale setup information with the corresponding illustration. When the geometrical information and simulation domain is updated, it is automatically synced with the REST API server

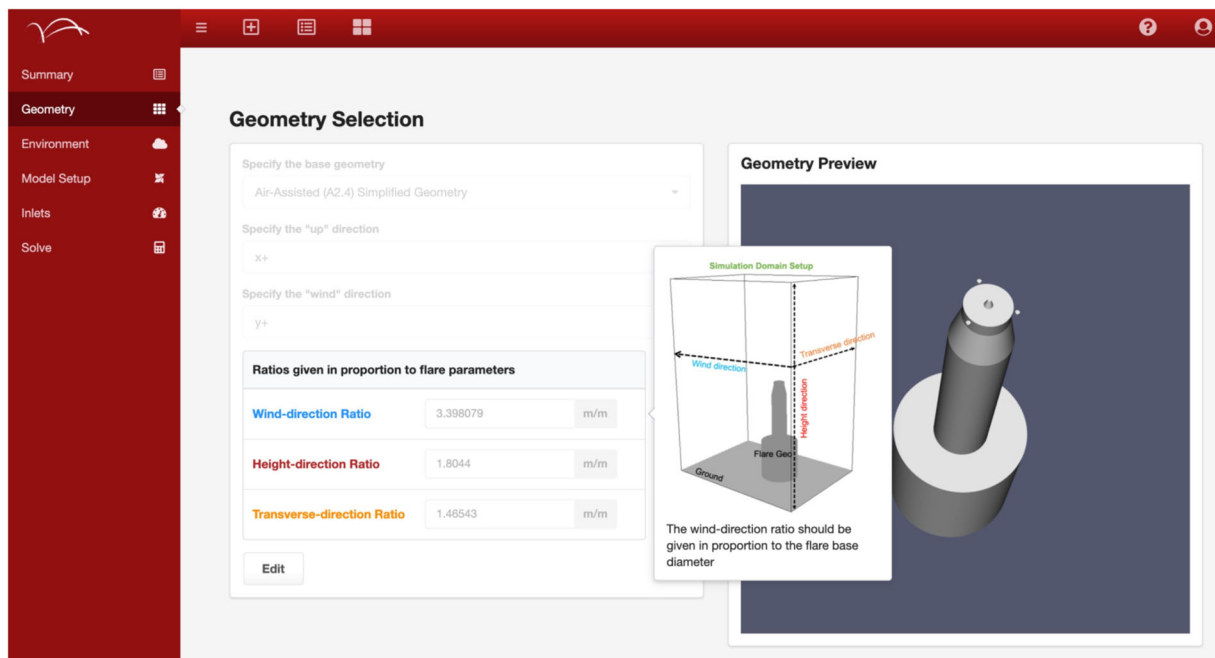


Figure 12: Geometry selection and preview page

### 3.2.2 Numerical simulation setup

This web interface allows the user to define the environmental conditions such as the wind speed, ambient temperature, and pressure, as is shown in Figure 13.

As shown in Figure 14, the interface allows the user to define various model parameters for the flare simulation setup, such as the mesh size, frequency of data collection and total physical time. Based on these model parameters, the FlaresUI estimates case-running parameters including residence time for the flow field, total number of cells, and the computational cost.

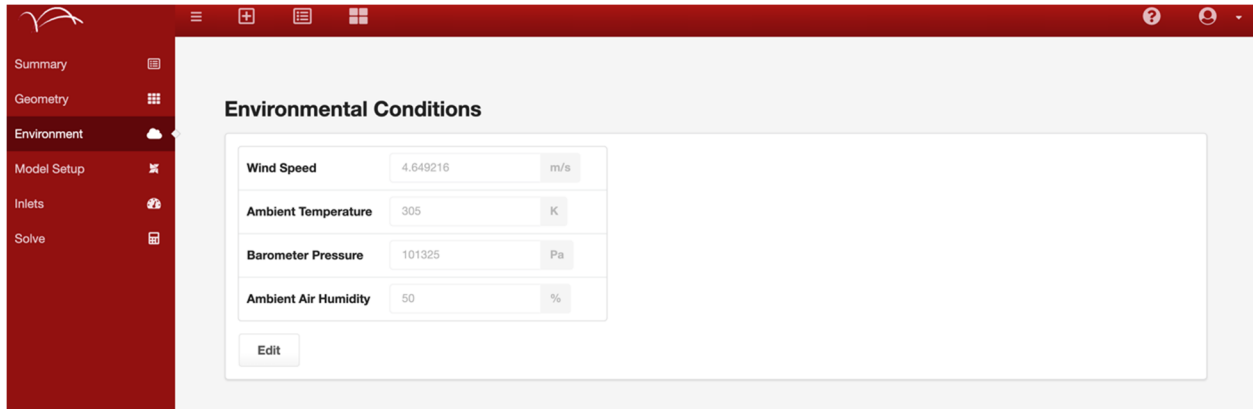


Figure 13: Environment conditions set-up page

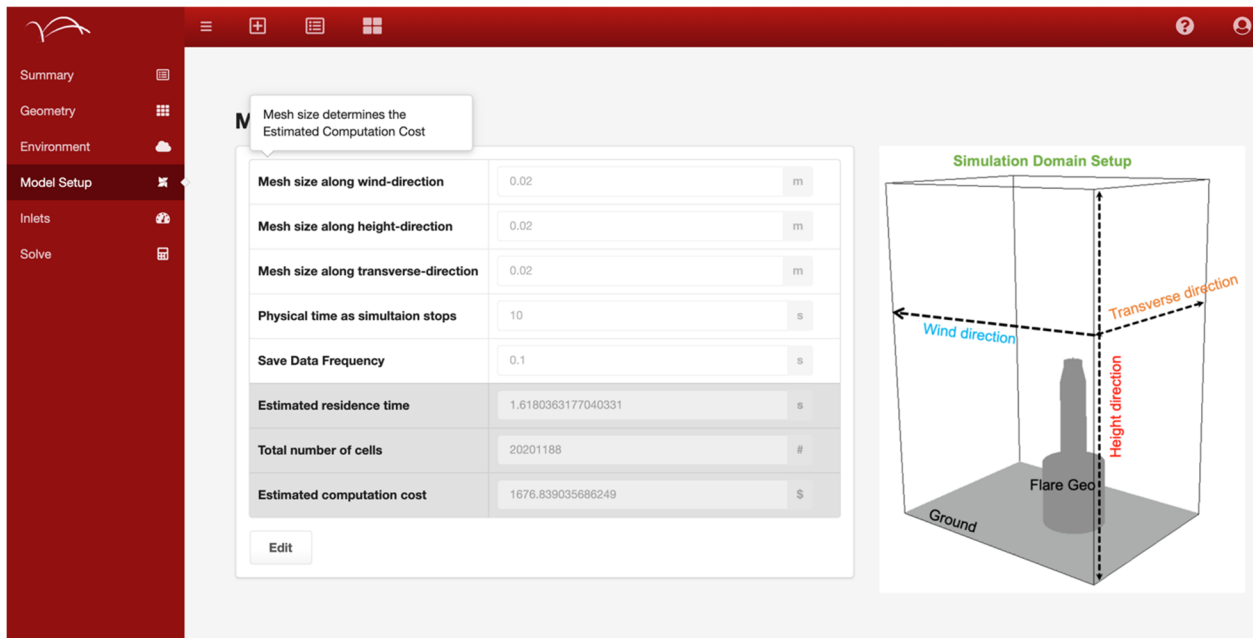


Figure 14: Flare simulation model set-up page

### 3.2.3 Inlet setup

As shown in Figure 15 15, multiple inlet types can be specified along with their chemical compositions, temperature, and mass flow rate. When in edit mode, the 3D rendering tool (also built with vtk.js) allows for the selection of the inlet faces by using the right mouse button (see the red and blue colored faces). These inlets are then used in conjunction with the CAD file to define the corresponding inlet boundary conditions.

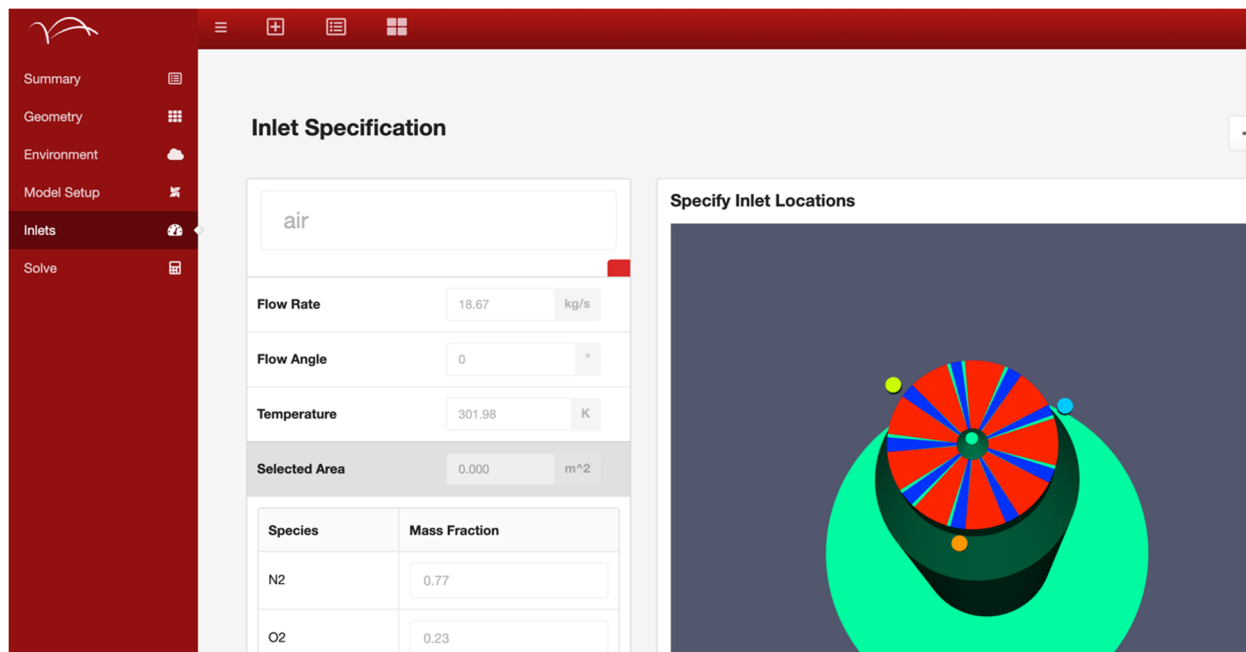


Figure 15: Inlet specification and selection page

### 3.2.4 Launching and Case Monitoring of Simulations

Currently, the UI includes capability for launching multiple flare simulations on the Nimbix cloud platform ([www.nimbix.net](http://www.nimbix.net)). This study has developed the monitoring abilities to the front-end web application. Additionally, simulation scalar and vector quantities can be queried at a given sampling frequency (e.g., temperature, velocity, pressure, etc.). These can be queried as the min/max values over the entire domain, or at specified lines or planes within the computational domain. Note that this type of monitoring is different than the full timestep data logging performed in Arches which is quite large and not feasible to pass back to the user in real time. The limited monitoring is orders of magnitude smaller in size and lends itself well to real time feedback for the user. The monitored data are specified *a priori* in the UPS file, and as the simulation proceeds, the data are output to custom text files on the remote compute device.

Custom Go code has been written in the HPC Lib to parse each of the unique output files for the monitored values. The data is parsed as it is generated by “tailing” the files (i.e., watching for changes). Once the data is parsed for a given quantity, it is packaged and sent to the REST API server and stored in the SQL database for a given solve. On the client side, the user interface continually asks the REST API server if new solve status information is available at regular

intervals. Once new data is available, the REST API server delivers it to the client. This gives the user the same feel as running a real time desktop application.

Additional React components have been developed for the user interface to display the monitoring results in a user-friendly graphical format. The plotting is based on the popular Recharts React component library [11]. An example of the prototype user interface is shown in Figure 16 with A2.4 running data. The plots are presented for multiple quantities and tabs are provided for switching between different variables and/or probing lines.

The evolution of Min-Max value and next  $\Delta t$  in the Case Status Section can indicate whether this simulation is proceeding in a stable fashion. If the case failed to launch or is not proceeding as expected, the user can decide to abort the simulation. The user can also define other local quantities of interest, such as combustion efficiency or temperature.

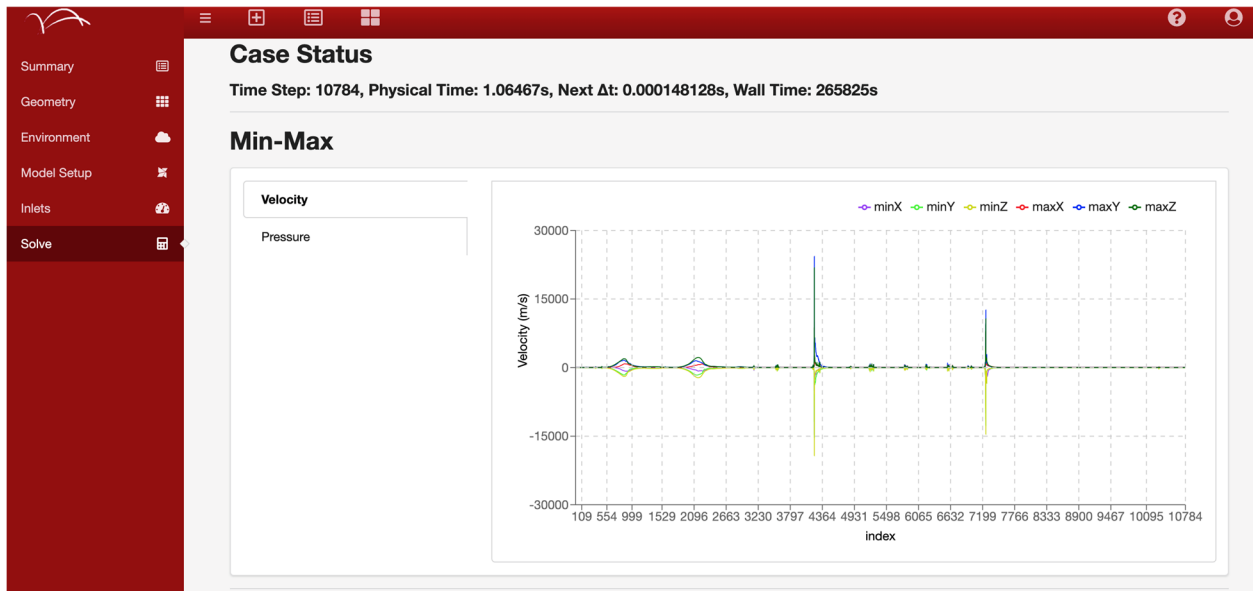


Figure 16: Case Monitoring window in the FlaresUI

## 4 Conclusions

The key objective of this research is to harden the UCF, particularly the Arches LES model component, to the commercial simulation of industrial flares. In this paper, our efforts have focused on two specific areas: 1) expanding the flare library to include two steam-assisted flare simulations, and 2) deployment of the web-interface. The two steam assist flare simulations, based on the 2010 TCEQ study, were completed and the predicted CE for case S2.1 was in close quantitative agreement with both the PFTIR, and GC based measurements. For case S2.3, with significantly higher flow rate of upper steam, the predicted CE was significantly reduced in qualitative agreement with the PFTIR and GC data. Although the predicted CE for this condition was in close quantitative agreement with the PFTIR measurements, the GC based measurements showed significantly lower CE. These types of differences within measurement data and between

measurements and predictions motivate the need for continuing verification and uncertainty quantification (VUQ) analysis (e.g. [2]).

The functionality of the web interface was demonstrated by setting up, simulating, monitoring, and post-processing the simulation of the air-assisted flare condition A2.4 from the 2010 TCEQ study. The interface provides capability to select from existing flare templates in the library, or to use the case-setup functionality to create a new case from scratch. The interface currently provides access to the Nimbix cloud platform, but future plans are to expand access to additional HPC providers.

## 5 Acknowledgement and Disclaimer

This material is based upon work supported by the U.S. Department of Energy, Office of Science, under Award Number DE-SC0017039.

This paper was prepared as an account of work sponsored by an agency of the United States Government. Neither the United States Government nor any agency thereof, nor any of their employees, makes any warranty, express or implied, or assumes any legal liability or responsibility for the accuracy, completeness, or usefulness of any information, apparatus, product, or process disclosed, or represents that its use would not infringe privately owned rights. Reference herein to any specific commercial product, process, or service by trade name, trademark, manufacturer, or otherwise does not necessarily constitute or imply its endorsement, recommendation, or favoring by the United States Government or any agency thereof. The views and opinions of authors expressed herein do not necessarily state or reflect those of the United States Government or any agency thereof.

The authors would like to acknowledge the Argonne Leadership Computing Facility for their allocation of core hours from their discretionary allotment.

## 6 Bibliography

- [1] M. Cremer, D. Wang and M. McGurn, "Leveraging the Uintah Computational Framework for Commercial Simulation of Industrial Flares," in *AFRC*, Salt Lake City, 2018.
- [2] M. Cremer, M. Zhou and D. Wang, J. Thornock, "Hardening of Arches for Commercial Simulation of Industrial Flares: Program Update," in *AFRC*, Virtual, 2020.
- [3] M. Cremer, M. Zhou, A. Cowley and D. Wang, "Progress Development of Arches for Commercial Simulation of Industrial Flares," in *AFRC*, Hawaii, 2019.
- [4] D. Castineira and T. F. Edgar, "CFD for simulation of steam-assisted and air-assisted flare combustion systems," *Energy & Fuels*, vol. 20, pp. 1044-1056, 2006.
- [5] D. T. Allen, "TCEQ 2010 Flare Study Final Report," The University of Texas at Austin, Texas, 2011.

- [6] O.L. Diaz, J. Spinti, B. Isaac, S. Smith and P. Smith, "A validation/uncertainty quantification analysis for a 1.5 MW oxy-coal fired furnace: Sensitivity analysis," *Journal of Verification, Validation and Uncertainty Quantification*, vol. 3, no. 1, pp. 1-15, 2018.
- [7] F. Nicoud, H. Toda, O. Cabrit, S. Boose and J. Lee, "Using singular values to build a subgrid-scale model for large eddy simulations," vol. 23, 2011.
- [8] P. Poudenx, *Plume Sampling of a Flare in crosswind: Structure and Combustion Efficiency*, Alberta : The University of Alberta, 2000.
- [9] [Online]. Available: <https://kitware.github.io/vtk-js/docs/index.html>.
- [10] J. Pohl and N. Soelbery, "Evaluation of the Efficiency of Industrial Flares: H<sub>2</sub>S Gas Mixture and Pilot assisted Flare," U.S Government Printing Office, Washington DC, 1986.
- [11] [Online]. Available: <http://recharts.org/en-US>.